RESEARCH ARTICLE

Rab34 small GTPase is required for Hedgehog signaling and an early step of ciliary vesicle formation in mouse

Shouying Xu[1,2], Yang Liu[1,3], Qing Meng[2,*] and Baolin Wang[1,4,*]

ABSTRACT

The primary cilium is a microtubule-based organelle that protrudes from the cell surface and plays essential roles in embryonic development. Ciliogenesis begins with the successive fusion of preciliary vesicles to form ciliary vesicles, which then dock onto the distal end of the mother centriole. Rab proteins have been linked to cilia formation in cultured cells, but not yet *in vivo*. In the present study, we demonstrate that endocytic recycling protein Rab34 localizes to cilia, and that its mutation results in significant decrease of ciliogenesis in both cultured cells and mice. Rab34 is required for the successive fusion of preciliary vesicles to generate ciliary vesicles and for the migration of the mother centriole from perinuclear region to plasma membrane. We also show that Rab34 mutant mice exhibit polydactyly, and cleft-lip and -palate. These phenotypes are consistent with observations that nonciliated Rab34 mutant cells fail to respond to Hedgehog signaling and that processing of full-length Gli3 to its C-terminally truncated form is reduced in Rab34 mutant embryos. Therefore, Rab34 is required for an early step of ciliary vesicle formation and Hh signaling *in vivo*.

This article has an associated First Person interview with the first author of the paper.

KEY WORDS: Rab34, Cilia, Ciliary vesicle, Hedgehog

INTRODUCTION

The primary cilium is a microtubule-based protrusion from the cell surface on most vertebrate cells. It is a sensory organelle and also a location for the transduction of many signaling molecules, including Hedgehog (Hh), Wnt and PDGF. Defects in ciliary structure and function are associated with a broad spectrum of developmental abnormalities and metabolic diseases, i.e. ciliopathies, such as open brain, holoprosencephaly, polydactyly, microphthalmia, cystic kidney disease and retinal degeneration, and can also result in obesity (Bangs and Anderson, 2017; Gerdes et al., 2009; Reiter and Leroux, 2017).

Most of developmental defects associated to ciliary gene mutation are attributed to impairment of Hh signaling between Smoothened (Smo) – a seven transmembrane G-protein-coupled receptor – and the transcription regulators Gli2 and Gli3 (Bangs and Anderson, 2017).

Proteolytic cleavage of the full-length Gli2 and Gli3 transcriptional activators (Gli2^{FL} and Gli3^{FL}, respectively) into their C-terminally truncated transcriptional repressor forms (Gli2^{Rep} and Gli3^{Rep}, respectively) is attenuated and, although activities of Gli2^{FL} and Gli3^{FL} are reduced, their levels are increased. Moreover, because the patterning of the central nervous system and limb in vertebrates is dependent on the correct ratio of Gli2^{FL}/Gli3^{FL} activators to Gli2^{Rep}/Gli^{Rep}, most of ciliary gene mutations – unsurprisingly – cause abnormalities in the central nervous system and limb development.

Ciliogenesis starts with the docking of the mother centriole (also known as basal body) to a ciliary vesicle (Sorokin, 1962), which results from the successive fusion of many small preciliary vesicles near the basal body, a process that requires Ehd1 (Lu et al., 2015). Following docking, the capping protein Cp110 (officially known as CCP110) is removed from the distal end of the mother centriole (according to observations using cultured cells; Schmidt et al., 2009; Spektor et al., 2007), and the basal body extends an axoneme that invaginates the vesicle (Sánchez and Dynlacht, 2016). During and after the process of vesicle docking and axoneme extension, the basal body migrates close to the plasma membrane from the perinuclear area. The vesicle then fuses with the plasma membrane to expose the cilia to the extracellular environment.

The cilia assembly requires vesicular trafficking that brings lipids and membrane proteins to the cilia membrane. The BBSome, an octameric protein complex that comprises seven Bardet–Biedl syndrome (BBS) proteins as well as BBIP1, functions as a coat complex required for sorting of specific membrane proteins to the primary cilia and is required for ciliogenesis (Jin et al., 2010). This ciliogenic function is thought to be mediated, at least in part, by its binding to the guanine nucleotide exchange factor (GEF) for Rab8 – Rabin8 (Nachury et al., 2007). Studies in cultured cells by using overexpression of Rab proteins and RNA interference (RNAi) of Rab RNA expression have demonstrated that the vesicular trafficking is dependent on Rab small GTPases, in particular the Rab11–Rab8 cascade (Knodler et al., 2010; Nachury et al., 2007; Westlake et al., 2010; Yoshimura et al., 2007). In this cascade, Rabin8 (which is enriched at the mother centriole) binds to Rab11 (also enriched at the mother centriole) and, subsequently, activates Rab8, which localizes to cilia and the basal body, to promote ciliary assembly. Surprisingly, however, Rab8 is dispensable for ciliogenesis *in vivo*, as Rab8a-Rab8b double-knockout mice display normal cilium morphology, length and number. Furthermore, the cilia in these double-mutant mice appear to be functionally normal, as no ciliopathies are detected (Sato et al., 2014). Unlike Rab8, mutations in Rab23 do result in ligand-independent activation of the Hh pathway (Eggenschwiler et al., 2001). This is because Rab23 regulates the transport of Kif17 (a kinesin that binds Gli2 and Gli3, and negatively regulates their activity) into cilia (Lim and Tang, 2015). Rab23 also maintains ciliary steady state of Smo (Boehlke et al., 2010). Nevertheless, cilia form normally in Rab23 mutant mice (Fuller et al., 2014) and, so far, no Rab proteins have been

[1]Department of Genetic Medicine, Weill Medical College of Cornell University, 1300 York Avenue, W404, New York, NY 10065, USA. [2]Institute of Biological Sciences and Biotechnology, Donghua University, Shanghai 201620, China. [3]Department of Veterinary Public Health, College of Veterinary Medicine, Jilin University, Jilin 130000, China. [4]Department of Cell and Developmental Biology, Weill Medical College of Cornell University, 1300 York Avenue, W404, New York, NY 10065, USA.

*Authors for correspondence (baw2001@med.cornell.edu; mengqing@dhu.edu.cn)

B.W., 0000-0002-2366-4980

linked to ciliogenesis *in vivo*. In addition, no Rab GTPases have been shown to regulate the fusion of preciliary vesicles to generate ciliary vesicles – even in cultured cells.

Rab34 is a Golgi-associated small GTPase (Wang and Hong, 2002). Loss of Rab34 has been recently shown to result in polydactyly in mice (Dickinson et al., 2016). While this manuscript was being reviewed, a large-scale CRISPR screen study reported that Rab34 is associated with ciliogenesis and Hh signaling in cultured cells (Pusapati et al., 2018). However, no *in vivo* study and mechanism were presented. We show in this study that Rab34 localized to cilia and that loss of Rab34 resulted in a significant decrease in ciliogenesis in mice. By using transmission electron microscopy (TEM), our study reveals that Rab34 is required for the successive fusion of small preciliary vesicles to form ciliary vesicles and for the migration of the mother centriole from the perinuclear area to the plasma membrane. Consistent with the defect in ciliogenesis, we also found Hh signaling impaired and Gli3 processing reduced in Rab34 mutant mice. This altered the ratio of Gli3^{FL} activator to Gli3 repressor (Gli3^{Rep}) and, consequently, caused polydactyly in Rab34 mutants. In support of the impairment of Hh signaling, Rab34 mutant mice exhibited cleft lip and cleft palate. Therefore, Rab34 is required for ciliogenesis and Hh signaling *in vivo*, and the fusion of preciliary vesicles to form ciliary vesicles.

RESULTS
Rab34 is required for ciliogenesis *in vivo*
A recent report has shown that a Rab34 mutation results in polydactyly in mice (Dickinson et al., 2016). Given that many known mutations of ciliary genes affect limb patterning due to reduced levels of the Gli3 repressor (Bangs and Anderson, 2017), we explored the possibility that Rab34 is involved in ciliogenesis. First, the *Rab34* gene was mutated in NIH3T3 cells by using CRISPR gene editing with two independent single-guide (sg) RNAs specifically targeting the *Rab34* gene (Rab34 sgRNA1 and Rab34 sgRNA2; see Materials and Methods) and a control sgRNA for green fluorescent protein (GFP). Heterogeneous populations of NIH3T3 cells transduced with lentivirus expressing either of the two sgRNAs together with Cas9 were then subjected to immunostaining for the ciliary marker Arl13b. The results showed that ~90% of GFP sgRNA NIH3T3 cells formed cilia, whereas only ~30% of the Rab34 sgRNA1 cells and <20% of Rab34 sgRNA2 cells developed cilia. Analysis of clonal Rab34 sgRNA2 NIH3T3 cells, which carried a large deletion in the gene (Fig. S1), showed a similar number of ciliated cells (Fig. 1A). Similar results were also obtained using C3H10T1/2 cells (Fig. S2).

To confirm the reduced ciliogenesis was specifically due to mutations in *Rab34*, a rescue experiment was performed. For this purpose, a FLAG- and streptavidin (FS)-tagged Rab34 cDNA mutant expression construct (FS-Rab34CR) was created. This mutant construct should be resistant to targeting by Rab34 sgRNA2 because nucleotide mutations created in the region corresponding sgRNA2 destroyed the sgRNA2 PAM sequence – amino acid residues, however, were unchanged. Stable overexpression of FS-Rab34CR in clonal Rab34 sgRNA2 NIH3T3 cells restored ciliogenesis of the mutant cells (Fig. 1A), indicating that reduced ciliogenesis in Rab34 sgRNA2 NIH3T3 cells is specifically due to mutations in the Rab34 gene.

To determine whether Rab34 is required for ciliogenesis *in vivo*, a Rab34 mutant mouse line was generated by deleting exons 2–6 in a targeted gene knockout approach. The deletion was confirmed by both Southern blotting (Fig. S3A,B) and RT-PCR (Fig. S3C); it removed the Rab34 genomic sequence [amino acid (aa) residues

19–171] from the 256 aa full-length protein and caused a reading frame shift, if exon 1 were spliced to exon 8 (Fig. S3A). Therefore, the mutant allele is most likely null. To determine whether the Rab34 mutant mice form cilia, the neural tube and limb bud sections of both wild-type (WT) and mutant embryos at embryonic day 10.5 (E10.5) were immunostained for ciliary markers Arl13b and acetylated tubulin. The results showed that cilium density in both tissues was significantly reduced. Only 5% of mutant primary mouse embryonic fibroblasts (pMEFs) formed cilia, as compared to >60% in WT (Fig. 1B). Thus, Rab34 is required for ciliogenesis *in vivo*.

Rab34 is required for Hh signaling and limb patterning but not neural tube patterning
Mice heterozygous for Rab34 mutant did not exhibit any noticeable abnormal phenotypes. Approximately 25% of E18.5 embryos examined were homozygous, and they were all alive (Table 1). However, no newborn homozygotes were alive, indicating that Rab34 mutant mice died around birth. Rab34 mutant embryos exhibited polydactyly and cleft lip and palate (Fig. 2A and Table 1) and occasionally exencephaly (*n*=1/21). This is consistent with defects in Hh signaling. However, heart, lung and liver of Rab34 mutant embryos appeared to be morphologically normal (data not shown), and heart looping was also normal (Table S1). Thus, the lethality of Rab34 mutant newborns was most likely due to functional defects of a vital organ(s). Since ciliary gene mutations often disrupt Hh signaling, we wanted to know in more detail whether Hh signaling is affected in the Rab34 mutant.

First, neural tube patterning along the anterior and posterior axis of embryos was assessed by examining the specification and patterning of neuronal markers that are regulated by Sonic Hedgehog (Shh) expressed in the notochord and floor plate (Briscoe et al., 2000). Foxa2, Nkx2.2 and Hb9 mark the floor plate, V3 and motoneuron progenitors, respectively, and are specified and patterned by Shh signaling. In contrast, Pax6 is a dorsal marker for Hh signaling and neural tube patterning, and is ventrally restricted by low levels of Shh signaling. Surprisingly, all these markers were specified and appeared to be patterned normally in Rab34 mutant embryos (Fig. 2B).

Second, since most ciliary gene mutations affect the processing of Gli3^{FL} to Gli3^{Rep} and of Gli2^{FL} levels, Gli3^{FL} and Gli3^{Rep} were examined by western blotting, showing that levels of both Gli2^{FL} and Gli3^{FL} were increased. However, levels of Gli3^{Rep} were decreased in mutant compared to the WT Rab34 mice (Fig. 2C), indicating that Gli3^{Fl} to Gli3^{Rep} processing is reduced in the mutant.

Third, to more directly determine whether loss of Rab34 affects Hh signaling, the RNA levels of *Ptch1* and *Gli1*, two direct Hh targets (Goodrich et al., 1996; Marigo et al., 1996), were examined by RT-qPCR before and after WT and Rab34 mutant pMEFs were stimulated with SAG, a synthetic Smo agonist (Chen et al., 2002). The results showed that, although stimulation with SAG upregulated *Ptch1* and *Gli1* RNA levels ~6- and 13-fold in WT cells, it did not so in the mutant cells (Fig. 2D), indicating that Hh signaling was impaired.

Smo and Gli2 accumulate in cilia upon Hh signaling (Chen et al., 2009; Corbit et al., 2005; Haycraft et al., 2005; Rohatgi et al., 2007; Wen et al., 2010). Since a small number of mutant pMEFs still form cilia, we were curious whether stimulation with SAG leads to the accumulation of Smo and Gli2 in cilia. Surprisingly, the percentage of Smo- or Gli2-positive cilia increased in both WT and Rab34 mutant cells in a dose-dependent manner, although it appeared to reach the maximum after stimulation with 100 nM SAG
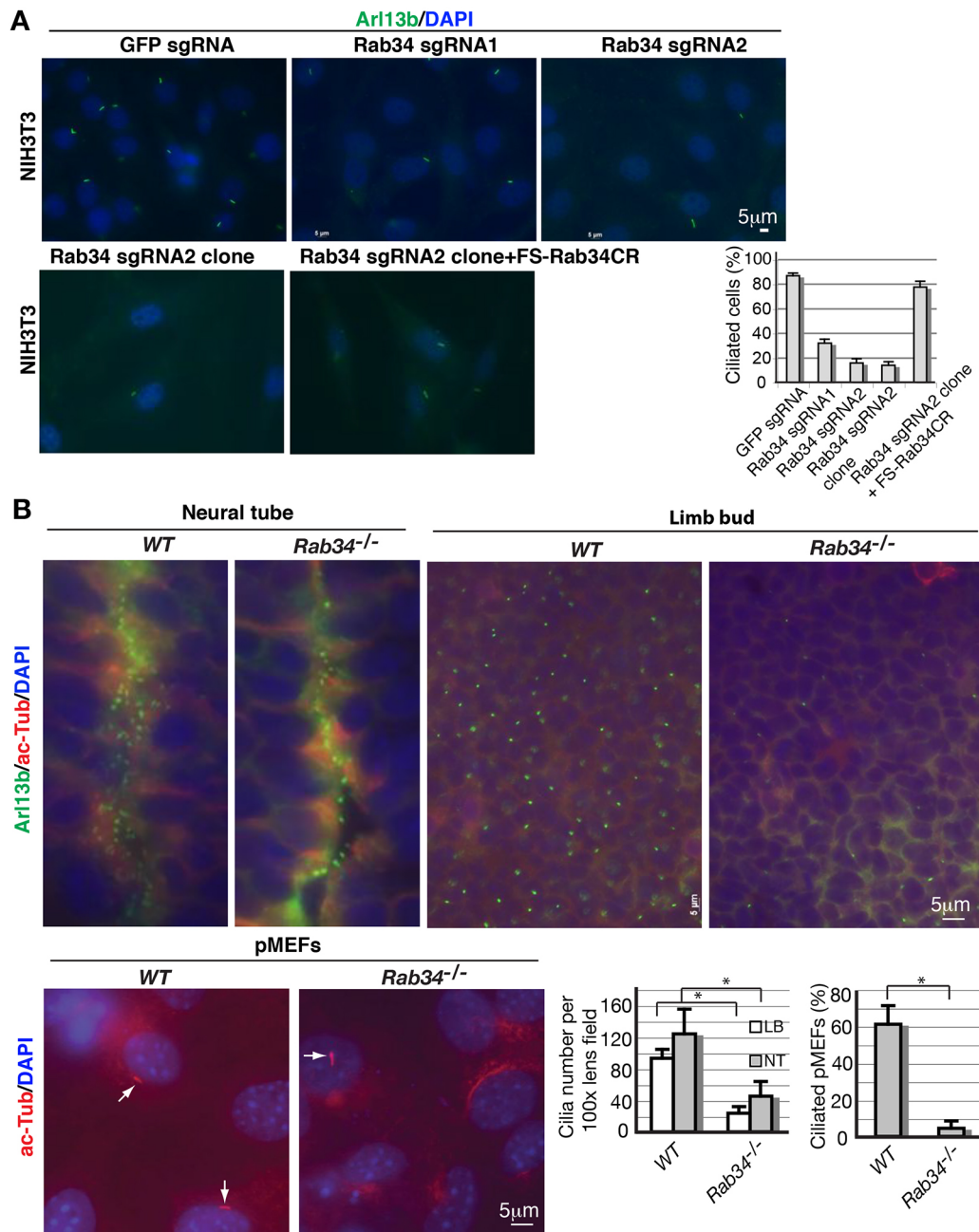
Fig. 1. Rab34 is required for ciliogenesis in both cultured cells and *in vivo*. (A) Loss of Rab34 in cultured cells results in a significant decrease in ciliogenesis. NIH3T3 cells were stably infected with lentivirus that expressed sgRNAs as indicated. The cells were then immunostained for the ciliary marker Arl13b and counterstained with DAPI (nuclei). (Top) heterogeneous cell populations; (bottom) clonal cells, with clonal cells expressing FS-Rab34CR (right). The graph shows that the percentage of ciliated cells was significantly reduced in cells expressing Rab34 sgRNA1 or Rab34 sgRNA2, as compared to control GFP sgRNA. Ciliogenesis of clonal Rab34 sgRNA2 cells is rescued by overexpression of FS-Rab34CR. Two-tailed Student's *t*-test $P \leq 0.00028$ ($n=3$ independent experiments, ≥ 100 cells counted for each category). (B) Loss of Rab34 results in a significant reduction in ciliogenesis in mouse tissues. Neural tube and limb bud sections at the forelimb area, and pMEFs of WT and Rab34 mutant were stained for the indicated ciliary markers. Graphs show the quantification of cilium numbers. Two-tailed Student's *t*-test $P \leq 0.000587$ ($n=5$ neural tube sections from two different embryos were counted); *, significantly different.

(Fig. 3A-C). The percentages for mutant cells varied substantially because of the small number of ciliated cells that could be found. Thus, the difference between WT and mutant following stimulation with a certain dose of SAG seemed to be statistically significant, whereas it did not with another dose. Nevertheless, the results indicate that these ciliated mutant cells are still capable of responding to Hh signaling, at least based upon accumulation of Smo and Gli2 in cilia. Similar results were observed for Smo in clonal Rab34 sgRNA2 NIH3T3 cells (Fig. 3D,E). Taken together,

these results suggest that Hh signaling is impaired in nonciliated, but not in ciliated, Rab34 mutant cells and that Hh signaling is not reduced enough to impact the neural tube patterning, presumably because some of neuroepithelial cells in the neural tube still develop cilia.

Rab34 localizes to cilia

Rab34 has been previously shown to localize to the Golgi complex (Wang and Hong, 2002). Given its role in ciliogenesis, we wondered

Table 1. E18.5 Rab34 embryos

Phenotype	Genotype			Total
	+/+	+/−	−/−	
	15	25	14	54
Preaxial polydactyly	0	0	14	14
Cleft lip and cleft palate	0	0	14	14
Viable	15	25	14	54

whether Rab34 also localized to cilia and/or the basal body. To that end, NIH3T3 cells that stably expressed LAP-Rab34WT fusion protein (GFP- and S-tagged Rab34WT) or LAP alone were created and subjected to co-staining for GFP and acetylated tubulin. The LAP-Rab34WT fusion protein localized to cilia in ∼25%

LAP-Rab34WT-expressing cells, whereas LAP alone localized diffusely in the cytoplasm and nucleus (Fig. 4A,B).

Rab proteins in the cell exist in an either GDP-bound (inactive) or GTP-bound (active) form. We, therefore, created the two mutant constructs LAP-Rab34T66N and LAP-Rab34Q111L that mimic the inactive and active form, respectively. Interestingly, only active LAP-Rab34Q111L but not the dominant-negative inactive LAP-Rab34T66N localized to cilia (Fig. 4A,B). This suggests that Rab34 is dependent on GTP-binding to either enter or reside in cilia. Given the role of Rab34 in ciliogenesis, we also wondered whether overexpression of Rab34 or of its mutants would promote ciliogenesis. Surprisingly, unlike the Rab8–Rab11 cascade (Knodler et al., 2010; Nachury et al., 2007; Yoshimura et al., 2007), it neither promoted nor inhibited ciliogenesis in NIH3T3 cells
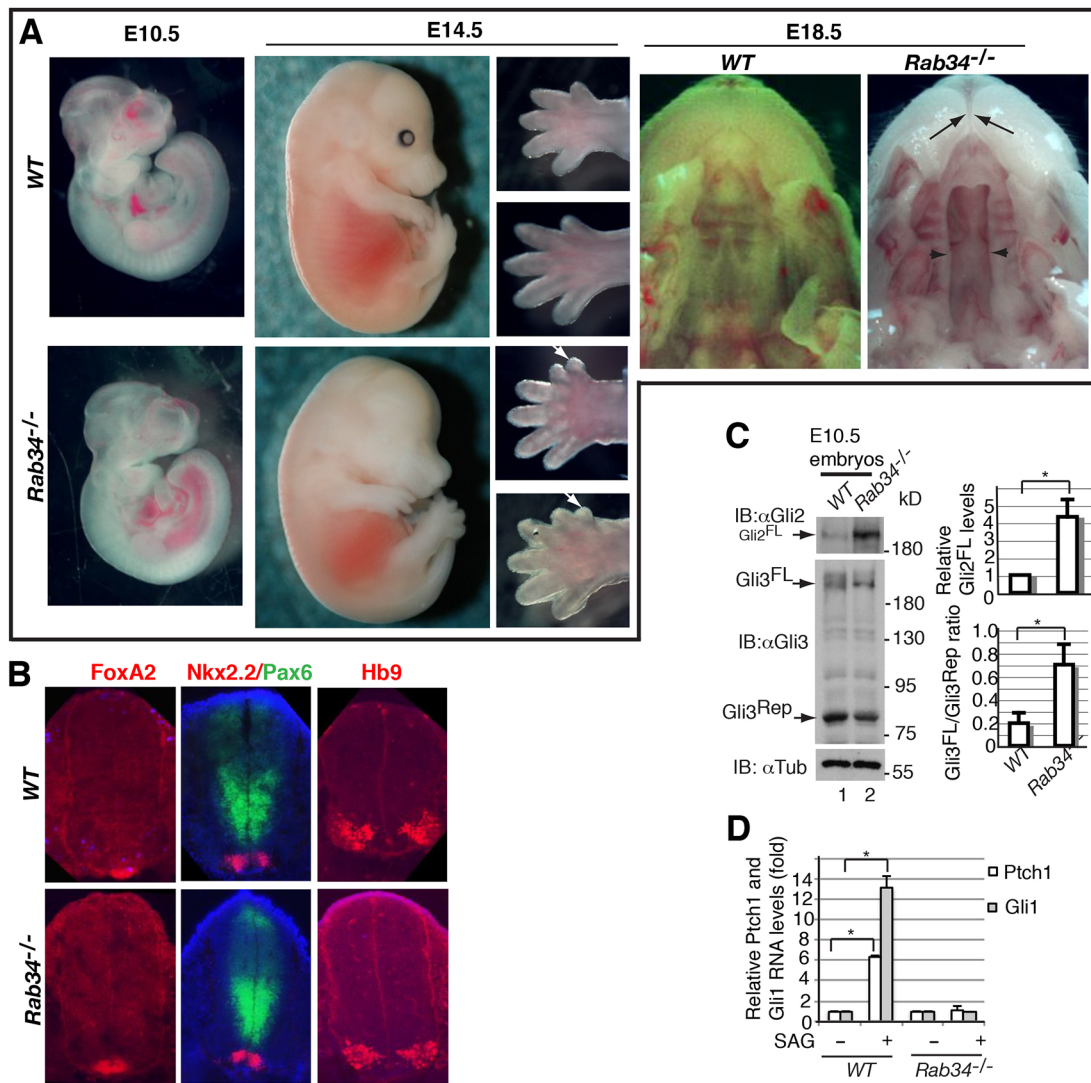

Fig. 2. Rab34 mutant mice exhibit polydactyly, cleft lip and palate, and reduced Hh signaling. (A) WT and Rab34 mutant embryos display polydactyly, and cleft lip and palate. For E14.5 embryos, arrows indicate extra digits. Lack of pigment in eyes of Rab34 mutant embryos is due to the segregation of albino from dark pigment, as heterozygous animals were maintained on a mixed albino SW and C57BL/6 background. For E18.5 embryos, arrows and arrowheads indicate cleft lip and palate, respectively. (B) Neural tube patterning is unaffected in Rab34 mutants. The neural tube sections around the forelimb areas of E10.5 embryos were stained for neuronal markers as indicated. All four markers appear to be specific, showing the normal pattern. For each genotype, ≥6 sections per marker and ≥3 embryos were used. (C) Gli3 processing is reduced in the Rab34 mutant. Western blot showing the levels of Gli2^{FL}, Gli3^{FL}, Gli3^{Rep} and α-tubulin (a loading control). Quantification is shown in the bar graphs to the right. Two-tailed Student's t-test P≤0.0115 (n=3 blots from 3 embryos). (D) Gli1 and Ptch1 RNA expression is not upregulated in Rab34 mutant pMEFs in response to stimulation with SAG. RT-qPCR shows relative RNA levels of Gli1 and Ptch1 in WT and Rab34 mutant pMEFs with or without stimulation with SAG. Two-tailed Student's t-test P=0.00001 for both Gli1 and Ptch1 (n=3 independent experiments); *, significantly different.
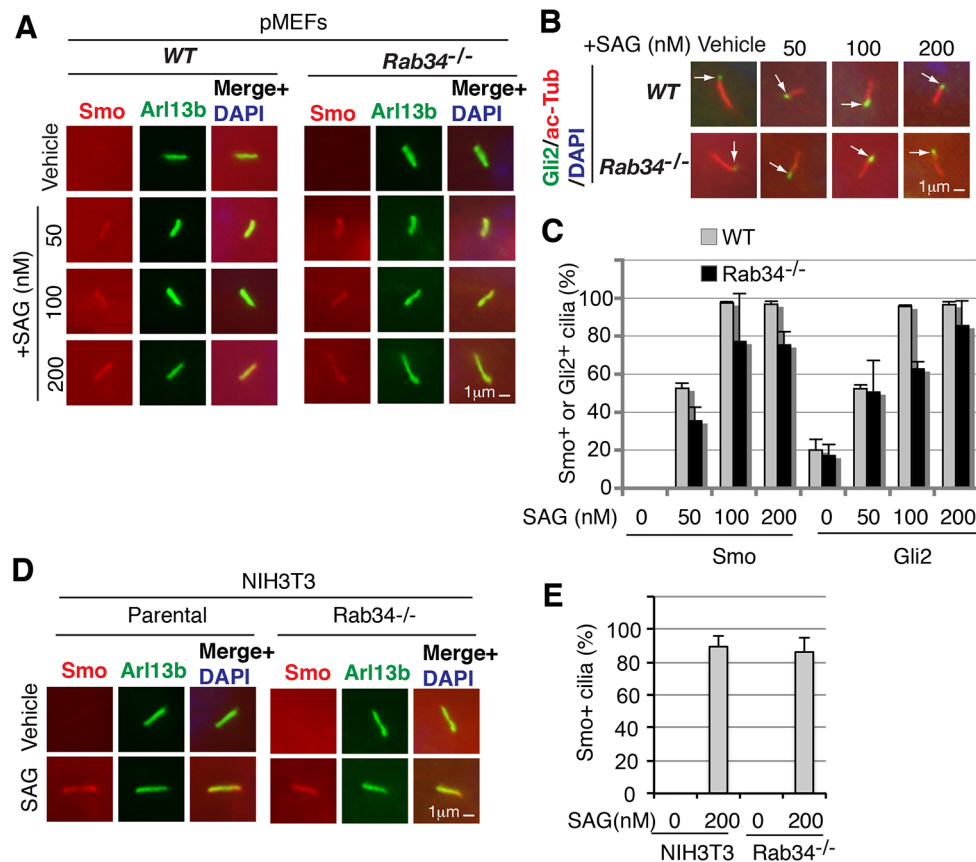
Fig. 3. Ciliated Rab34 mutant pMEFs and NIH3T3 cells are capable of responding to stimulation with the Smo agonist SAG. WT and Rab34 mutant pMEFs were incubated with vehicle or various concentrations of SAG overnight, and were then subjected to immunostaining of proteins as indicated above the panels (A) or to the left (B). Arrows indicate Gli2 staining in cilia. (C) Bar graph, showing quantification of data from three independent experiments. Note that both Smo and Gli2 accumulate in cilia of mutant cells upon stimulation with SAG. Two-tailed Student's *t*-test *P* values between WT and mutant are 0.018, 0.235, 0.007 (Smo at 50, 100, 200 nM SAG) and 0.862, 0.001, 0.222 (Gli2 at 50, 100, 200 nM SAG) (*n*=3 independent experiments; in each category ≥100 cilia for WT and ≥10 cilia for mutant were counted). The large variation in the mutant is due to the small number of cilia being found. The overall trend is that that ciliated mutant cells show slightly weaker response to SAG stimulation compared to WT cells. (D) After overnight incubation with vehicle or SAG (200 nM), parental and Rab34 mutant NIH3T3 cells were stained for Smo and Arl13b. Note that Smo accumulated in cilia upon treatment with SAG in both parental and mutant cells. (E) The graph shows data from 3 independent experiments (≥130 cilia for WT and ≥11 cilia for mutant were counted for each experiment).

(Fig. 4A,B). It is worth noting that LAP-Rab34T66N was less stable than LAP-Rab34WT (Fig. 4C). Thus, its inability to inhibit ciliogenesis is probably partially due to its low expression level.

Centrosomal and ciliary localizations of Rab8, Rab11, BBS4, IFT20 and Cp110 are independent of Rab34

Studies with cultured cells using overexpression and RNAi showed that the Rab8–Rab11 cascade is required for ciliogenesis (Knodler et, al., 2010; Nachury et al., 2007; Westlake et al., 2010; Yoshimura et al., 2007). Consistent with this, Rab8 localizes to cilia and the centrosome, and Rab11 is enriched in the centrosome (Knodler et al., 2010; Nachury et al., 2007; Westlake et al., 2010; Yoshimura et al., 2007). Given the role of Rab34 in ciliogenesis, we next wanted to know whether loss of Rab34 affects subcellular localization of Rab8, Rab11 and Rabin8. To this end, LAP-tagged Rab8, Rab11 and Rabin8 were stably overexpressed in either parental or Rab34 mutant NIH3T3 cells, and then subjected to immunostaining for GFP and γ-tubulin (marking centrioles), or for GFP and acetylated α-tubulin (marking cilia). The results showed that the centrosomal and ciliary localizations of none of these proteins were altered in the mutant cells (Fig. 5).

BBS4 is a part of the BBSome and localizes to centrioles and its satellite matrix; the BBSome functions as a coat complex and is required for sorting of specific membrane proteins to the primary cilia (Jin et al., 2010; Nachury et al., 2007). IFT20 is a subunit of anterograde IFT-B complex and localizes to both centrioles and Golgi network (Follit et al., 2006). Since Rab proteins are essential for membrane vesicle sorting, we wondered whether the subcellular localization of the BBSome and IFT20 are affected by loss of Rab34. However, immunostaining results showed that their subcellular localization in Rab34 mutant cells was similar to those in WT cells and, thus, independent of Rab34 (Fig. 5).

Ehd1 localizes to the ciliary pocket and regulates the fusion of preciliary vesicles in order to form ciliary vesicles (Lu et al., 2015). As expected, overexpressed LAP-Ehd1 was found in parts of cilia near the basal body (presumably the cilium pocket) and in the cytoplasm of WT pMEFs. However, it localized diffusely to the cytoplasm without accumulation at the basal body in Rab34 mutant Rab34 pMEFs (Fig. 5), suggesting that Ehd1 is not recruited to the mother centrioles in mutant cells.

Overexpression and RNAi studies using cultured mammalian cells have shown that Cp110 is a capping protein at the distal end of centrioles and is removed from the mother centrioles during an early step of ciliogenesis (Schmidt et al., 2009; Spektor et al., 2007). Our staining results indicated that Cp110 was properly removed from the mother centrioles in Rab34 mutant cells, as evidenced by the presence of Cp110 signals only at daughter centrioles in most
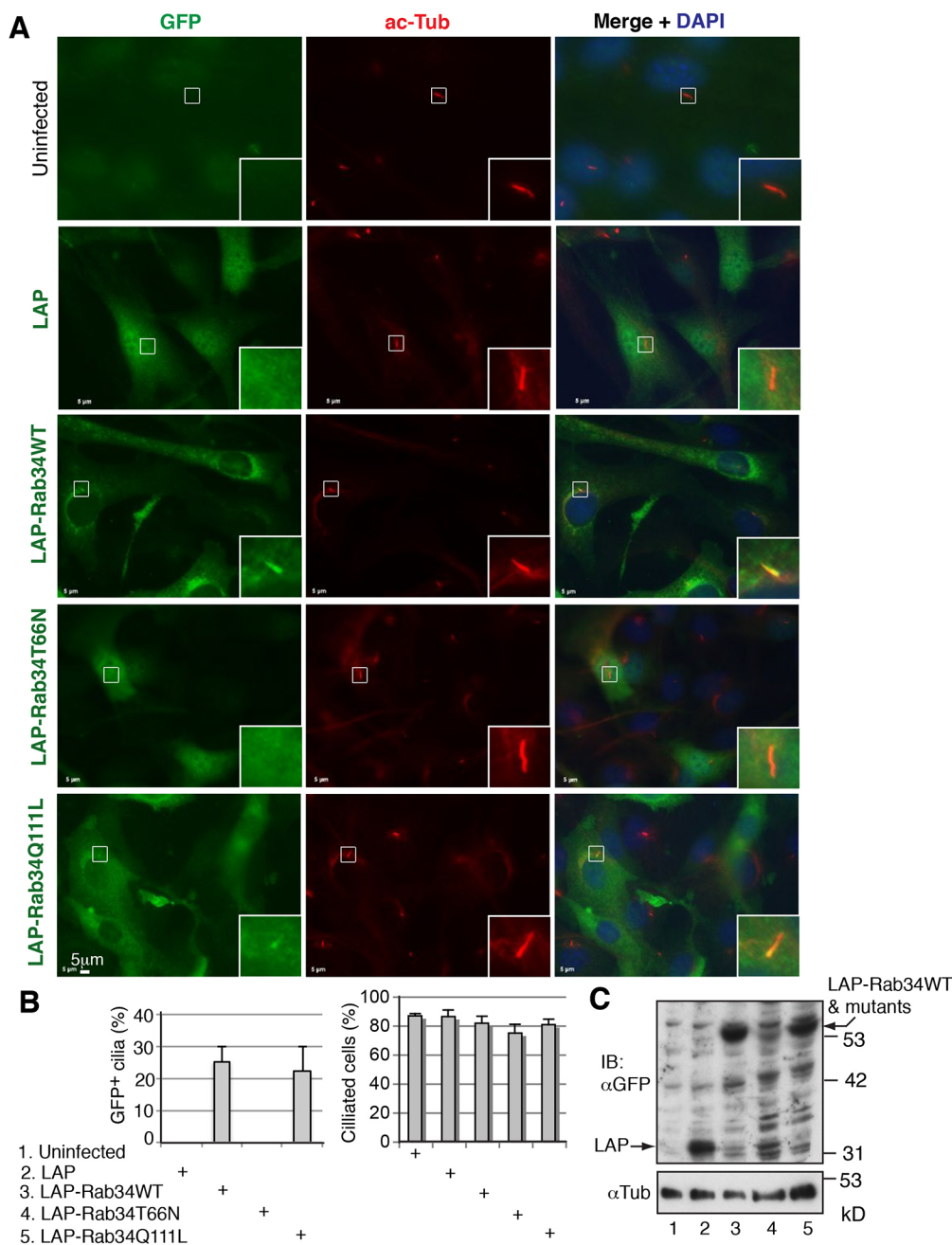
Fig. 4. Rab34 localizes to cilia but its overexpression is not sufficient to promote ciliogenesis. (A) NIH3T3 cells stably expressing the indicated fusion proteins were stained for GFP, acetylated tubulin (ac-Tub) and DAPI (nucleus). Insets on right are enlargement (5x) of boxed area. (B) Graphs showing the quantitative staining results. Note that LAP-Rab34WT and LAP-Rab34Q111L (active mutant) but not LAP or LAP-Rab34T66N (dominant-negative inactive mutant), localized to cilia in >20% of cells that express either fusion protein (graph on left). However, overexpression of either LAP-Rab34WT or LAP-Rab34Q111L is not sufficient to induce ciliogenesis (graph on right), because two-tailed Student's t-test $P \geq 0.0565$ ($n \geq 240$ cells for each category). + indicates fusion proteins corresponding to columns. (C) Western blot showing expression of LAP and LAP-Rab34WT and mutants. α-Tubulin (αTub) was used as a loading control. Lane number corresponds to proteins in B.

mutant cells (Fig. 5). Thus, loss of Rab34 does not affect the removal of Cp110 from the mother centriole.

Loss of Rab34 leads to the accumulation of preciliary vesicles

Ciliogenesis begins with successive fusion of preciliary vesicles to form ciliary vesicles; these then dock onto distal appendages of the mother centrioles, followed by assembly of the transition zone and axoneme and fusion of ciliary vesicles with the plasma membrane (Sánchez and Dynlacht, 2016). During and after the process of axoneme initiation and elongation, mother centrioles need to migrate from the perinuclear region to near the plasma membrane so that, once ciliary vesicles fuse with the plasma membrane, the mother centriole is tethered to the plasma membrane.

To better understand which step in ciliogenesis was affected by loss of Rab34, the ultrafine structure of cilia on the neuroepithelial progenitors in the neural tube of both WT and mutant embryos was examined by using TEM. Micrographs were divided into five categories according to the state of mother centrioles: (1) mother centrioles not anchored to plasma membrane but surrounded by preciliary vesicles, (2) mother centrioles anchored to plasma membrane and surrounded by preciliary vesicles, (3) mother centrioles docked to ciliary vesicles, (4) mother centrioles with elongated axoneme and, (5) mother centrioles alone. In mutant cells 43.2% of mother centrioles were not anchored to the plasma membrane but surrounded by many preciliary vesicles, whereas, in WT cells only 5.7% of mother centrioles fell into this category. Similarly, 11.1% of mother centrioles in mutant cells showed elongated axonemes, whereas in WT 32% did. This is consistent with our observations of reduced ciliogenesis using immunostaining (Fig. 1B). In addition, we also observed that the percentage of mother centrioles anchored to the plasma membrane in WT embryos
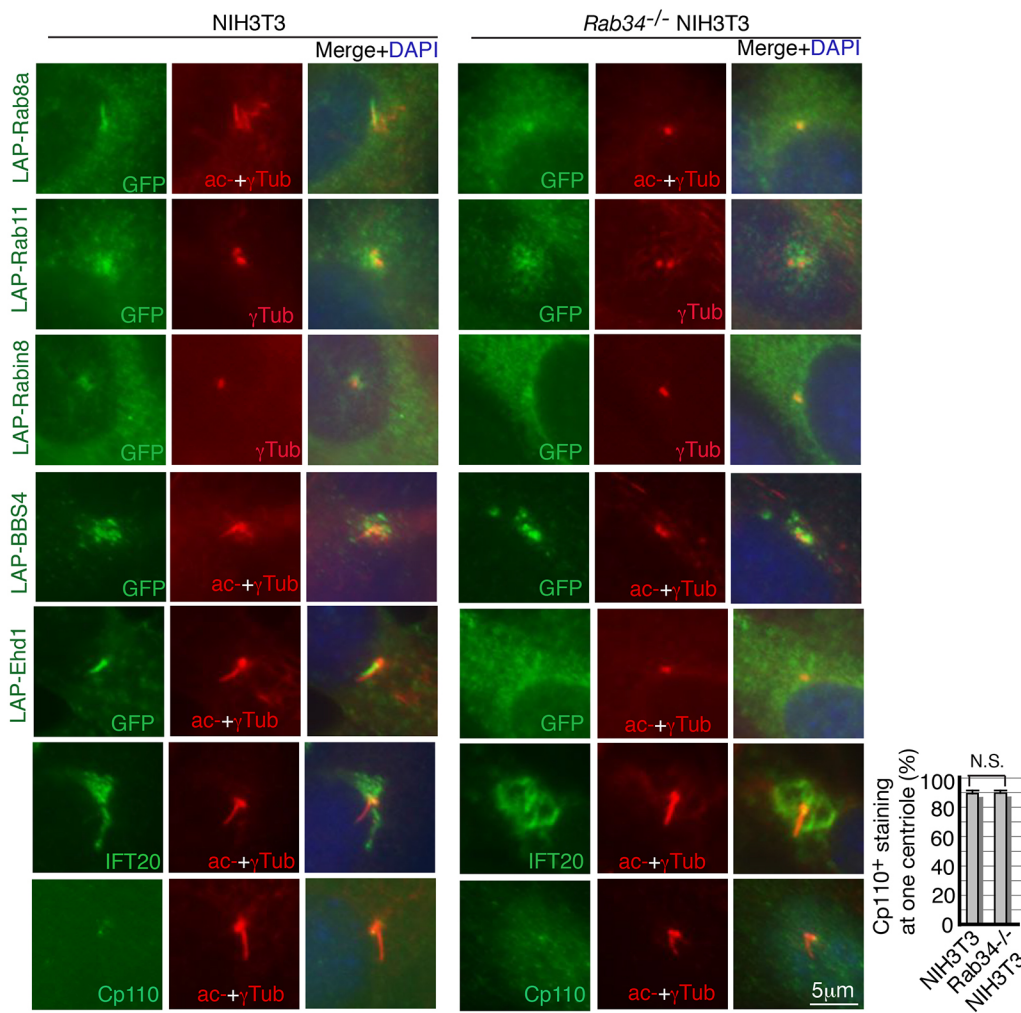
Fig. 5. Rab34 is not required for centrosomal and/or ciliary localization of Rab8, Rab11, Rabin8, BBS4, IFT20 and Cp110. WT NIH3T3 and Rab34 mutant NIH3T3 cells, and these cells overexpressing the indicated LAP fusion proteins were stained as indicated for GFP, endogenous proteins (IFT20 and Cp110), γ-tubulin (γTub) or acetylated and γ-tubulin (ac-+γTub) together. Ciliated cilia were selected for IFT20 and CP110, and a general population of cells was used for other markers. For each protein, except CP110, ≥10 images were taken. Note that the centriolar and ciliary localizations of all proteins examined are independent of Rab34. Graph on the right shows quantification of Cp110 staining at one centriole; two-tailed Student's t-test P=0.816 (n≥54 cells). N.S., not significant.

was markedly higher than that in the mutant (11.3% vs 1.2%) (Fig. 6A and B). Together, these results suggest that Rab34 regulates the successive fusion of preciliary vesicles to form ciliary vesicles and the migration of the mother centrioles from perinuclear area to plasma membrane.

DISCUSSION

Here we show that loss of Rab34 results in a significant decrease in ciliogenesis in both cultured pMEFs and mouse tissues (Fig. 1). The decreased ciliogenesis consequently disrupts Hh signaling and causes Hh-related phenotypes (Fig. 2). Thus, Rab34 is required for both ciliogenesis and Hh signaling.

There are two pieces of evidence that Hh signaling is impaired in Rab34 mutants. First, the levels of Gli2^{FL} protein are increased and Gli3^{FL} processing is reduced in Rab34 mutant (Fig. 2C). The latter alters the ratio of Gli3^{FL} to Gli3^{Rep}, which explains why Rab34 mutant displays polydactyly (Fig. 2A). Second, RT-qPCR results demonstrate that the expression of *Ptch1* and *Gli1* RNAs, two direct Hh targets, fails to respond to Smo activation following treatment with SAG in Rab34 mutant pMEFs (Fig. 2D). These observations resemble those in other known ciliary gene mutants (Bangs and Anderson, 2017).

However, it was unexpected that the neural tube patterning appears to be generally normal in the Rab34 mutant (Fig. 2B). A similar phenotype has also recently reported in a *Dzip1l* ciliary gene mutant (Lu et al., 2017; Wang et al., 2018). Since neural tube patterning is largely dependent on Gli2^{FL} activator activity,

this finding suggests that the Gli2^{FL} activator function is not significantly affected in the neural tube of Rab34 mutants.

It is even more surprising that a small number of Rab34 mutant pMEFs and NIH3T3 cells both still develop cilia and that these ciliated cells appear to be able to respond to stimulation with SAG on the basis of the accumulation of both Smo and Gli2 in cilia (Fig. 3). This suggests that Rab34 is dispensable for ciliogenesis of these cells because either these cells do not normally express Rab34 or, if they do, there are another Rab protein(s) that compensate the loss of Rab34 function. Given that a small number of Rab34 mutant NIH3T3 cells, which are presumably homogenous, remain ciliated, the latter is more likely. While this manuscript was being revised, a large-scale CRISPR mutagenesis study uncovered that Rab34 mutations affect ciliogenesis of NIH3T3 cells. However, the study showed that Smo fails to be enriched in the cilia of Rab34 mutant cells upon stimulation with SAG (Pusapati et al., 2018). The discrepancy between that study and ours is probably due to the sensitivity of different Smo antibodies or a variation of NIH3T3 cells used in two studies.

A genome-wide chromosomal immunoprecipitation (ChIP) study identified Rab34 to be a potential transcriptional target of Gli transcription factors (Vokes et al., 2007). However, our RT-qPCR analysis showed that Rab34 RNA expression in pMEFs was not significantly upregulated upon stimulation with SAG (Fig. S4). Thus, additional studies are needed to determine whether Rab34 is a true Hh target or not.
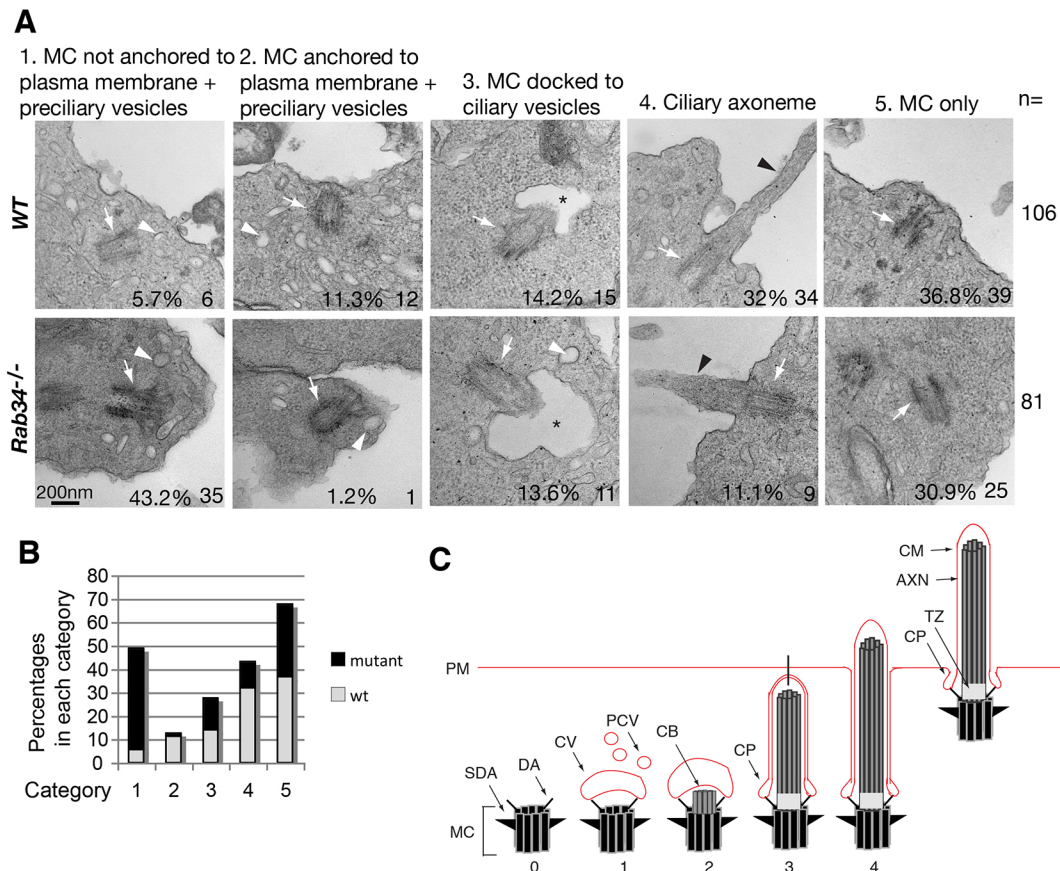
Fig. 6. Rab34 regulates the successive fusion of preciliary vesicles to form ciliary vesicles and migration of the basal bodies to cell cortex. (A) TEM micrographs of cilia on neuroepithelial cells in the neural tube near the forelimb area of E10.5 embryos of the indicated genotype (one embryo for each). Mother centrioles (MCs) are indicated by arrows, cilia are indicated by black arrowheads, representative preciliary vesicles are indicated by white arrowheads, ciliary vesicles are indicated by asterisks. The percentage and number of mother centrioles in each category are stated within each micrograph; the total number of images (n) is given on the right of the panel. (B) The graph compares WT and mutant for each category. (C) Diagram showing the processes of cilia formation. Membrane structure is depicted in red. MC, mother centriole; DA, distal appendage; SDA, subdistal appendage; CV, cilia vesicle; PCV, periciliary vesicle; CB, cilia bud; CP, ciliary pocket; TZ, transition zone; AXN, axoneme; CM, cilia membrane; PM, plasma membrane.

Both Rab34wt and Rab34Q111L localize to cilia only in a small fraction of overexpressed cells (Fig. 4). However, Rab34T66N does not. This suggests that GTP binding is required for Rab34 to be localized in cilia. Since both Rab34wt and Rab34Q111L exhibit the similar ability to be localized in cilia, GTP binding is probably required only for the protein to enter but not reside in cilia.

Studies in cultured cells by using overexpression and RNAi approaches have linked Rab8-Rab11 cascade to ciliogenesis (Knodler et al., 2010; Nachury et al., 2007; Westlake et al., 2010; Yoshimura et al., 2007). However, an *in vivo* study has demonstrated that Rab8 is dispensable for ciliogenesis, as cilia are formed normally in *Rab8a* and *Rab8b* double mutant mice (Sato et al., 2014). Similarly, cell culture studies have suggested that Rab23 is involved in ciliogenesis (Lim and Tang, 2015; Yoshimura et al., 2007), but the *in vivo* evidence does not support that (Eggenschwiler et al., 2001; Fuller et al., 2014). Thus, to our knowledge, no Rab proteins have been so far linked to ciliogenesis *in vivo* and Rab34 is the first one shown to be required for ciliogenesis *in vivo*.

Ciliogenesis begins with the successive fusion of preciliary vesicles to form ciliary vesicles, which dock onto the distal appendages of the mother centrioles, followed by the formation of the transition zone and initiation and elongation of axoneme (Sánchez and Dynlacht, 2016). During and after the initiation and

elongation of axoneme, the mother centrioles must migrate close to plasma membrane from the perinuclear area so that ciliary vesicles can fuse with plasma membrane to expose cilia to extracellular space. A study that used TEM to investigate RNAi of Ehd1 in RPE cells showed that endocytic recycling protein Ehd1 is required for successive fusion of preciliary vesicles to form ciliary vesicles (Lu et al., 2015). In our present study, we show that Rab34 also appears to regulate this process, as there was a marked accumulation of preciliary vesicles in Rab34 mutant (43.2% mother centrioles surrounded by preciliary vesicles in the mutant versus 5.7% in WT). More interestingly, there were fewer basal bodies anchored to the plasma membrane and surrounded by preciliary vesicles in the Rab34 mutant compared with those in WT embryos (1.2% vs 11.3%) (Fig. 6A and B). Thus, Rab34 appears to regulate the making of ciliary vesicles from preciliary vesicles and the migration of the basal bodies to cell cortex.

It is currently unclear how loss of Rab34 results in preciliary vesicle accumulation. Rab34 does not seem to function through Rab8-Rab11 cascade, as the ciliary and/or centriolar localizations of Rab8, Rab11 and Rabin8 are independent of Rab34 (Fig. 5). It does not also appear to act via BBS4 and IFT20, since their subcellular localization is unaffected in the absence of Rab34 (Fig. 5). The relationship between Rab34 and Ehd1 with respect of ciliary vesicle formation is also not clear. Because the vast majority of Rab34

mutant NIH3T3 cells and pMEFs cannot form cilia, and because we could not obtain an antibody that recognizes endogenous Ehd1, we were unable to determine whether Ehd1 ciliary localization is dependent on Rab34 (Fig. 5). Nevertheless, Ehd1 siRNA knockdown appears to impair the recruitment of IFT20 to the mother centrioles and the removal of Cp110 from the mother centrioles (Lu et al., 2015), whereas the subcellular localization of both proteins appears to be normal in Rab34 mutant cells (Fig. 5). This suggests that Rab34 and Ehd1 are likely to act in different steps to regulate the fusion of preciliary vesicles to generate ciliary vesicles. Additional studies are necessary to understand the relationship between Rab34 and Ehd1 in ciliogenesis.

MATERIALS AND METHODS
Generation of a Rab34 mutant allele
Institutional Animal Care and Use Committee at Weill Cornell Medical College approved this research, including the use of mice and mouse embryonic fibroblasts.

A BAC clone containing C57BL/6J mouse Rab34 genomic DNA sequences was purchased from the BACPAC Resources Center (Oakland, CA) and used to create a Rab34-targeting construct. The construct was engineered by replacing exons 2–6 of the *Rab34* gene with the neomycin cassette flanked by loxP sites (Fig. S3A). The linearized construct was electroporated into W4 mouse embryonic stem (ES) cells (129S6/SvEvTac), and targeted ES cell clones were identified by digestion of genomic DNA with Acc65I, followed by Southern blot analysis of ES cell DNA using a probe as indicated (Fig. S3B). Two Rab34-targeted ES cell clones were injected into C57BL/6 blastocysts to generate chimeric founders, which were then bred with Swiss Webster (SW) outbred mice to establish F1 heterozygotes and maintain the mouse colony. PCR analysis was used for routine genotyping with the following primers: forward primer BW1901F1, 5′-CTTCCAGATAGCCTTGTCATC-3′ and reverse primer BW1901R, 5′-CTCTTAGACTTCCTGCATTCC-3′ for WT allele, which produced a 260 bp fragment; and forward primer BW294, 5′-ATTGGGAAGACAA-TAGCAGGC-3′ and BW1901R for the targeted *Rab34* allele, which produced a 230 bp fragment. The primers used for RT-PCR to confirm Rab34 mutant allele were BW1645F, 5′-CTGTGGGGAAGACCTGTCT-CATTAAT-3′ on exon 4, and BW1646R, 5′-TGAACCTTTCCTGACCA-GCCGTGTCC-3′ on exon 5.

Cell lines and cell culture
WT and mutant Rab34 primary mouse embryonic fibroblasts (pMEFs) were prepared from E13.5 or E14.5 mouse embryos. pMEFs in the first passage were used for this study. HEK293, C3H10T1/2 and pMEFs were cultured in DMEM supplemented with 10% fetal bovine serum (FBS), penicillin and streptomycin. NIH3T3 and its derived cells were cultured in DMEM supplemented with 10% calf serum, penicillin and streptomycin. The stable cell lines were established by transducing NIH3T3 cells with lentivirus carrying the designated constructs and then selecting clones resistant to puromycin (3 µg/ml) (Santa Cruz Biotechnology).

Generation of Rab34 mutant cells using CRISPR
DNA oligonucleotides used to express single-guide (sg) RNAs specific for GFP and Rab34 were: sgRNA GFP, forward 5′-caccGAGCTGGACGGC-GACGTAAA-3′ and reverse 5′-aaacTTTACGTCGCCGTCCAGCTC-3′; Rab34 sgRNA1, forward 5′-caccGCCTGCCAGGAGCACCGGAC-3′, reverse aaacGTCCGGTGCTCCTGGCAGGC; and Rab34 sgRNA2, forward 5′-caccGCGGAGGGAGGGACCGCGTCCTGG-3′ and reverse 5′-aaac-CCAGGACGCGGTCCCTCCGC-3′. The nucleotides in lower case letters were used for cloning the double oligonucleotides into BsmBI site of pLenti-Crispr-v2 vector, Addgene plasmid #52961 (deposited by Feng Zhang; Sanjana et al., 2014). To generate lentivirus, each of the resulting constructs was transfected into HEK293 cells together with packaging plasmids: pMD2.G and psPAX2, Addgene plasmids #12259 and #12260 (deposited by Didier Trono) using the calcium phosphate precipitation method (Wang et al., 2013). NIH3T3 and C3H10T1/2 cells were transduced

with lentivirus by using medium containing lentivirus and polybrene (4 µg/ml) overnight, followed by selection with puromycin (3 µg/ml). Single Rab34 sgRNA2 clones were selected by a limited dilution of puromycin-resistant clones in 96-well plates. The mutations were identified by nested PCR using primers BW1648F 5′-CGGATCAGGCCTCTGCGCCTTC-3′, BW1648R1 5′-GCGGCCTCTTTCTTCAGGCAC-3′, BW1648R2 5′-CT-GAGAGGAACATTGTGAGAAT-3′, followed by digestion with PflF1 and DNA sequencing. The mutant clone used for the study contains a 51 bp deletion at the junction of the first exon and intron, which destroys RNA splicing (Fig. S1).

cDNA constructs, cloning, transfection and virus transduction
Rab34, Rab8, Rab11, Rabin8 and BBS4 cDNAs were amplified by PCR using a mouse cDNA library and specific primers for these cDNAs. Rab34T66N and Rab34Q111L were generated by overlap extension PCR using primers carrying respective point mutations. pENTR-LAP and pENTR-FS were engineered by inserting either a localization and affinity purification (LAP) tag (GFP and S double tags) or FS (FLAG and streptavidin double tags) into the pENTR4(686-1) vector. All LAP-tagged fusion constructs were created by inserting the indicated cDNAs into pENTR-LAP and then moving the LAP-cDNAs into pLenti-CMV-puro DEST vector by using LR-Clonase II (Thermo Scientific). pLenti-FS-Rab34 construct was created by inserting Rab34 into the pENTR-FS vector followed by moving it into pLenti-CMV-puro DEST vector using LR-Clonase II. The CRISPR-resistant FS-Rab34 construct FS-Rab34CR was created by a PCR-based mutagenesis method using pENTR-FS-Rab34 as a template and primers BW1970F (5′-GACCGCGTaCTGGCa GAGCTGCCC-3′) and BW1970R (5′-GGGCAGCTCtGCCAGtACG CGGTC-3′), in which the nucleotides in lower case indicate mutations. This avoids targeting by sgRNA2 without altering the amino acid sequence of Rab34. All constructs created by PCR were sequenced. pENTR4(686-1) and pLenti-CMV-Puro DEST(w118-1) were Addgene plasmids #17424 and #17452 (deposited by Eric Campeau and Paul Kaufman; Campeau et al., 2009). The LAP-Ehd1 construct was a gift from Christopher Westlake (Lu et al., 2015). The generation and transduction of lentivirus is described above.

Preparation of embryo sections, immunofluorescence and microscopy
For immunofluorescence of neural tube sections, mouse embryos at 10.5 days post coitus (E10.5) were dissected, fixed in 4% paraformaldehyde (PFA)/PBS for 1 h at 4°C, equilibrated in 30% sucrose/PBS overnight at 4°C and embedded in OCT. The frozen embryos were transversely cryosectioned (10 µm/section). Tissue sections around fore- and hind-limb areas were immunostained using antibodies against Foxa2 (concentrated), Nkx2.2, Hb9 [Developmental Study Hybridoma Bank (DSHB), Iowa] and Pax6 [Biolegend, #PRB-278P), or against Arl13b together with anti-acetylated tubulin antibody as described (Pan et al., 2009).

For cell ciliation studies, cells were plated on coverslips that had been coated with 0.1% gelatin for at least overnight and serum-starved with 0.1% FBS for 20–24 h to arrest the cells. For centrosome staining, cells were fixed with cold (−20°C) methanol for 5 min. For cytoplasmic and cilium staining, cells were fixed in 4% PFA/PBS for 15 min. For both centrosome and cilium staining, cells were fixed in 4% PFA for 2 min and then cold methanol for 5 min. After a wash (3×) with PBS, the cells were incubated with blocking solution (PBS, 0.2% Triton X-100, 2% heat-inactivated calf serum) for 20 min. The cells were then incubated with primary antibodies in blocking solution for 1 h at room temperature. In some cases, the fixed cells were incubated with PBS/0.2% Triton-X-100 for 5 min and then immediately with primary antibodies. The cells were washed with PBS and incubated with secondary antibodies in blocking solution for 1 h at room temperature. After washes in PBS (3×), the coverslips were mounted to glass slides using Vectashield mounting fluid supplemented with DAPI (Vector Labs). Staining was visualized using a Zeiss Axiovert fluorescent microscope.

Antibodies
Anti-Cp110 antibodies were generated by immunizing rabbits with a His-tagged Cp110 fragment (1-149 aa). Other antibodies include: anti-Gli2,

anti-Gli3, anti-Smo, anti-Arl13b and anti-GFP (all 1:1000) (Wang et al., 2000, 2013; Wu et al., 2017, 2014), as well as antibodies against acetylated tubulin (1:2000), γ-tubulin (1:4000) (Sigma) and IFT20 [1:500; a gift from Gregory J. Pazour (Pazour et al., 2002)]. Secondary antibodies Alexa Fluor 488-conjugated goat anti-rabbit IgG and Cy3-conjugated goat anti-mouse IgG were purchased from Jackson Immunoresearch, Inc.

Immunoblotting
E10.5 mouse embryos used to detect Gli2 or Gli3 were lysed in RIPA buffer (50 mM Tris-HCl pH 7.4, 150 mM NaCl, 1 mM EDTA, 1%Triton X-100, 1% sodium deoxycholate, 0.1% SDS, protease inhibitors). Stable NIH3T3 cells were lysed in lysis buffer (50 mM HEPES pH 7.4, 150 mM NaCl, 1 mM EDTA, 1% NP40, 10% glycerol, protease inhibitors). Immunoblotting was performed as described (Wang et al., 2000).

Transmission electron microscopy
E10.5 embryos were fixed with 2% paraformaldehyde/2.5% glutaraldehyde in 0.1 M sodium cacodylate buffer pH 7.4 (EM quality) overnight at 4°C. After washes with sodium cacodylate buffer (3×) and then water (3×), the fixed embryos were transversely cut into 5–6 segments. The segments were incubated with 1% OsO4 for 1 h in dark. After washing 3× with water, segments were incubated in 1% uranyl acetate for 2 h at room temperature, washed 3× with water and dehydrated with a series of graded ethanol. The embryo segments were then infiltrated and embedded with Embed812 mixed solution according to the manufacturer's instruction (Electron Microscopy Sciences, Inc.). Transverse ultrathin sections (65 nm) were cut with a Leica UC6 ultramicrotome (Leica Microsystems), stained with uranyl acetate and lead nitrate and imaged with a JEOL1400 transmission electron microscope.

Reverse transcription quantitative PCR
Confluent WT and Rab34-mutant pMEFs in 60 mm plates were incubated with growth medium containing SAG (200 nM; Cayman Chemical) or vehicle control overnight. Total RNA was isolated from the pMEFs by using TRIzol solution according to the manufacturer's instruction (Thermo Fisher Scientific). Of the isolated total RNAs, 5µg of each were used to synthesize first stranded cDNA using SuperScript II reverse transcriptase according to the manufacturer's instruction (Thermo Fisher Scientific). Reverse transcription quantitative PCR (RT-qPCR) was performed using a qPCR kit (MasterMix-R, Applied Biological Materials, Inc., Canada) and primers described previously (Wang et al., 2017). Primers for Rab34 were: BW1916F 5′-CCAAGAAGGACCTGAGTACTCCT-3′ and BW1916R 5′-TTCCCGGACATTCTCACCAGTGA-3′. For a 20 µl reaction, 0.15 µl of the first strand cDNA was used.

Author contributions
Conceptualization: B.W.; Methodology: S.X., Y.L., B.W.; Formal analysis: B.W.; Investigation: S.X., Y.L., B.W.; Writing - original draft: B.W.; Writing - review & editing: S.X., Q.M., B.W.; Supervision: Q.M., B.W.; Funding acquisition: Q.M., B.W.

Supplementary information
Supplementary information available online at
http://jcs.biologists.org/lookup/doi/10.1242/jcs.213710.supplemental

References
Bangs, F. and Anderson, K. V. (2017). Primary cilia and mammalian hedgehog signaling. *Cold Spring Harb. Perspect Biol.* **9**.

Boehlke, C., Bashkurov, M., Buescher, A., Krick, T., John, A.-K., Nitschke, R., Walz, G. and Kuehn, E. W. (2010). Differential role of Rab proteins in ciliary trafficking: Rab23 regulates smoothened levels. *J. Cell Sci.* **123**, 1460-1467.

Briscoe, J., Pierani, A., Jessell, T. M. and Ericson, J. (2000). A homeodomain protein code specifies progenitor cell identity and neuronal fate in the ventral neural tube. *Cell* **101**, 435-445.

Campeau, E., Ruhl, V. E., Rodier, F., Smith, C. L., Rahmberg, B. L., Fuss, J. O., Campisi, J., Yaswen, P., Cooper, P. K. and Kaufman, P. D. (2009). A versatile viral system for expression and depletion of proteins in mammalian cells. *PLoS ONE* **4**, e6529.

Chen, J. K., Taipale, J., Young, K. E., Maiti, T. and Beachy, P. A. (2002). Small molecule modulation of Smoothened activity. *Proc. Natl. Acad. Sci. USA* **99**, 14071-14076.

Chen, M.-H., Wilson, C. W., Li, Y.-J., Law, K. K. L., Lu, C.-S., Gacayan, R., Zhang, X., Hui, C.-C. and Chuang, P.-T. (2009). Cilium-independent regulation of Gli protein function by Sufu in Hedgehog signaling is evolutionarily conserved. *Genes Dev.* **23**, 1910-1928.

Corbit, K. C., Aanstad, P., Singla, V., Norman, A. R., Stainier, D. Y. R. and Reiter, J. F. (2005). Vertebrate Smoothened functions at the primary cilium. *Nature* **437**, 1018-1021.

Dickinson, M. E., Flenniken, A. M., Ji, X., Teboul, L., Wong, M. D., White, J. K., Meehan, T. F., Weninger, W. J., Westerberg, H., Adissu, H. et al. (2016). High-throughput discovery of novel developmental phenotypes. *Nature* **537**, 508-514.

Eggenschwiler, J. T., Espinoza, E. and Anderson, K. V. (2001). Rab23 is an essential negative regulator of the mouse Sonic hedgehog signalling pathway. *Nature* **412**, 194-198.

Follit, J. A., Tuft, R. A., Fogarty, K. E. and Pazour, G. J. (2006). The intraflagellar transport protein IFT20 is associated with the Golgi complex and is required for cilia assembly. *Mol. Biol. Cell* **17**, 3781-3792.

Fuller, K., O'Connell, J. T., Gordon, J., Mauti, O. and Eggenschwiler, J. (2014). Rab23 regulates Nodal signaling in vertebrate left-right patterning independently of the Hedgehog pathway. *Dev. Biol.* **391**, 182-195.

Gerdes, J. M., Davis, E. E. and Katsanis, N. (2009). The vertebrate primary cilium in development, homeostasis, and disease. *Cell* **137**, 32-45.

Goodrich, L. V., Johnson, R. L., Milenkovic, L., McMahon, J. A. and Scott, M. P. (1996). Conservation of the hedgehog/patched signaling pathway from flies to mice: induction of a mouse patched gene by Hedgehog. *Genes Dev.* **10**, 301-312.

Haycraft, C. J., Banizs, B., Aydin-Son, Y., Zhang, Q., Michaud, E. J. and Yoder, B. K. (2005). Gli2 and Gli3 localize to cilia and require the intraflagellar transport protein polaris for processing and function. *PLoS Genet.* **1**, e53.

Jin, H., White, S. R., Shida, T., Schulz, S., Aguiar, M., Gygi, S. P., Bazan, J. F. and Nachury, M. V. (2010). The conserved Bardet-Biedl syndrome proteins assemble a coat that traffics membrane proteins to cilia. *Cell* **141**, 1208-1219.

Knodler, A., Feng, S., Zhang, J., Zhang, X., Das, A., Peranen, J. and Guo, W. (2010). Coordination of Rab8 and Rab11 in primary ciliogenesis. *Proc. Natl. Acad. Sci. USA* **107**, 6346-6351.

Lim, Y. S. and Tang, B. L. (2015). A role for Rab23 in the trafficking of Kif17 to the primary cilium. *J. Cell Sci.* **128**, 2996-3008.

Lu, Q., Insinna, C., Ott, C., Stauffer, J., Pintado, P. A., Rahajeng, J., Baxa, U., Walia, V., Cuenca, A., Hwang, Y. S. et al. (2015). Early steps in primary cilium assembly require EHD1/EHD3-dependent ciliary vesicle formation. *Nat. Cell Biol.* **17**, 228-240.

Lu, H., Galeano, M. C. R., Ott, E., Kaeslin, G., Kausalya, P. J., Kramer, C., Ortiz-Bruchle, N., Hilger, N., Metzis, V., Hiersche, M. et al. (2017). Mutations in DZIP1L, which encodes a ciliary-transition-zone protein, cause autosomal recessive polycystic kidney disease. *Nat. Genet.* **49**, 1025-1034.

Marigo, V., Johnson, R. L., Vortkamp, A. and Tabin, C. J. (1996). Sonic hedgehog differentially regulates expression of GLI and GLI3 during limb development. *Dev. Biol.* **180**, 273-283.

Nachury, M. V., Loktev, A. V., Zhang, Q., Westlake, C. J., Peränen, J., Merdes, A., Slusarski, D. C., Scheller, R. H., Bazan, J. F., Sheffield, V. C. et al. (2007). A core complex of BBS proteins cooperates with the GTPase Rab8 to promote ciliary membrane biogenesis. *Cell* **129**, 1201-1213.

Pan, Y., Wang, C. and Wang, B. (2009). Phosphorylation of Gli2 by protein kinase A is required for Gli2 processing and degradation and the Sonic Hedgehog-regulated mouse development. *Dev. Biol.* **326**, 177-189.

Pazour, G. J., Baker, S. A., Deane, J. A., Cole, D. G., Dickert, B. L., Rosenbaum, J. L., Witman, G. B. and Besharse, J. C. (2002). The intraflagellar transport protein, IFT88, is essential for vertebrate photoreceptor assembly and maintenance. *J. Cell Biol.* **157**, 103-113.

Pusapati, G. V., Kong, J. H., Patel, B. B., Krishnan, A., Sagner, A., Kinnebrew, M., Briscoe, J., Aravind, L. and Rohatgi, R. (2018). CRISPR screens uncover

genes that regulate target cell sensitivity to the morphogen sonic hedgehog. *Dev. Cell* **44**, 113-129 e118.

Reiter, J. F. and Leroux, M. R. (2017). Genes and molecular pathways underpinning ciliopathies. *Nat. Rev. Mol. Cell Biol.* **18**, 533-547.

Rohatgi, R., Milenkovic, L. and Scott, M. P. (2007). Patched1 regulates hedgehog signaling at the primary cilium. *Science* **317**, 372-376.

Sánchez, I. and Dynlacht, B. D. (2016). Cilium assembly and disassembly. *Nat. Cell Biol.* **18**, 711-717.

Sanjana, N. E., Shalem, O. and Zhang, F. (2014). Improved vectors and genome-wide libraries for CRISPR screening. *Nat. Methods* **11**, 783-784.

Sato, T., Iwano, T., Kunii, M., Matsuda, S., Mizuguchi, R., Jung, Y., Hagiwara, H., Yoshihara, Y., Yuzaki, M., Harada, R. et al. (2014). Rab8a and Rab8b are essential for several apical transport pathways but insufficient for ciliogenesis. *J. Cell Sci.* **127**, 422-431.

Schmidt, T. I., Kleylein-Sohn, J., Westendorf, J., Le Clech, M., Lavoie, S. B., Stierhof, Y.-D. and Nigg, E. A. (2009). Control of centriole length by CPAP and CP110. *Curr. Biol.* **19**, 1005-1011.

Sorokin, S. (1962). Centrioles and the formation of rudimentary cilia by fibroblasts and smooth muscle cells. *J. Cell Biol.* **15**, 363-377.

Spektor, A., Tsang, W. Y., Khoo, D. and Dynlacht, B. D. (2007). Cep97 and CP110 suppress a cilia assembly program. *Cell* **130**, 678-690.

Vokes, S. A., Ji, H., McCuine, S., Tenzen, T., Giles, S., Zhong, S., Longabaugh, W. J. R., Davidson, E. H., Wong, W. H. and McMahon, A. P. (2007). Genomic characterization of Gli-activator targets in sonic hedgehog-mediated neural patterning. *Development* **134**, 1977-1989.

Wang, T. and Hong, W. (2002). Interorganellar regulation of lysosome positioning by the Golgi apparatus through Rab34 interaction with Rab-interacting lysosomal protein. *Mol. Biol. Cell* **13**, 4317-4332.

Wang, B., Fallon, J. F. and Beachy, P. A. (2000). Hedgehog-regulated processing of Gli3 produces an anterior/posterior repressor gradient in the developing vertebrate limb. *Cell* **100**, 423-434.

Wang, C., Low, W.-C., Liu, A. and Wang, B. (2013). Centrosomal protein DZIP1 regulates Hedgehog signaling by promoting cytoplasmic retention of transcription factor GLI3 and affecting ciliogenesis. *J. Biol. Chem.* **288**, 29518-29529.

Wang, C., Li, J., Meng, Q. and Wang, B. (2017). Three Tctn proteins are functionally conserved in the regulation of neural tube patterning and Gli3 processing but not ciliogenesis and Hedgehog signaling in the mouse. *Dev. Biol.* **430**, 156-165.

Wang, C., Li, J., Takemaru, K. I., Jiang, X., Xu, G. and Wang, B. (2018). Centrosomal protein Dzip1l binds Cby, promotes ciliary bud formation, and acts redundantly with Bromi to regulate ciliogenesis in the mouse. *Development* **146**, dev164236.

Wen, X., Lai, C. K., Evangelista, M., Hongo, J.-A., de Sauvage, F. J. and Scales, S. J. (2010). Kinetics of hedgehog-dependent full-length Gli3 accumulation in primary cilia and subsequent degradation. *Mol. Cell. Biol.* **30**, 1910-1922.

Westlake, C. J., Baye, L. M., Nachury, M. V., Wright, K. J., Ervin, K. E., Phu, L., Chalouni, C., Beck, J. S., Kirkpatrick, D. S., Slusarski, D. C. et al. (2010). Primary cilia membrane assembly is initiated by Rab11 and transport protein particle II (TRAPPII) complex-dependent trafficking of Rabin8 to the centrosome. *Proc. Natl. Acad. Sci. USA* **108**, 2759-2764.

Wu, C., Yang, M., Li, J., Wang, C., Cao, T., Tao, K. and Wang, B. (2014). Talpid3-binding centrosomal protein Cep120 is required for centriole duplication and proliferation of cerebellar granule neuron progenitors. *PLoS ONE* **9**, e107943.

Wu, C., Li, J., Peterson, A., Tao, K. and Wang, B. (2017). Loss of dynein-2 intermediate chain Wdr34 results in defects in retrograde ciliary protein trafficking and Hedgehog signaling in the mouse. *Hum. Mol. Genet.* **26**, 2386-2397.

Yoshimura, S., Egerer, J., Fuchs, E., Haas, A. K. and Barr, F. A. (2007). Functional dissection of Rab GTPases involved in primary cilium formation. *J. Cell Biol.* **178**, 363-369.

```
WT        10857   CGGATCAGGCCTCTGCGCCTTCCCGGGGAGCCCCGCAAGGCCGCAGACAAGATGAACATT   10916
                  ||||||||||||||||||||||||||||||||||||||||||||||||||||||||||||
Mutant    206     CGGATCAGGCCTCTGCGCCTTCCCGGGGAGCCCCGCAAGGCCGCAGACAAGATGAACATT   147
                                          Exon 2                      Intron
WT        10917   CTGGCGCCCGTGCGGAGGGACCGCGTCCTGGCGGAGCTGCCCCAGGTAGGCACCAGGGCC   10976
                  |||||                                                       |||
Mutant    146     CTGGC------------------------------------------------------GCC   139

WT        10977   ACGTCGGGCCTCTGGCTGTCGCTGAGTGTGGGCGGGGAGAAGGTGGCCCAGCCCCGTCGC   11036
                  ||||||||||||||||||||||||||||||||||||||||||||||||||||||||||||
Mutant    138     ACGTCGGGCCTCTGGCTGTCGCTGAGTGTGGGCGGGGAGAAGGTGGCCCAGCCCCGTCGC   79

WT        11037   CCTGCAAGGCCCGCTGCTCCTGGGTGGTCCGCTTCCCACCCCACCCCCAGCCCAGGGCTG   11096
                  ||||||||||||||||||||||||||||||||||||||||||||||||||||||||||||
Mutant    78      CCTGCAAGGCCCGCTGCTCCTGGGTGGTCCGCTTCCCACCCCACCCCCAGCCCAGGGCTG   19

WT        11097   CT   11098
                  ||
Mutant    18      CT   17
```

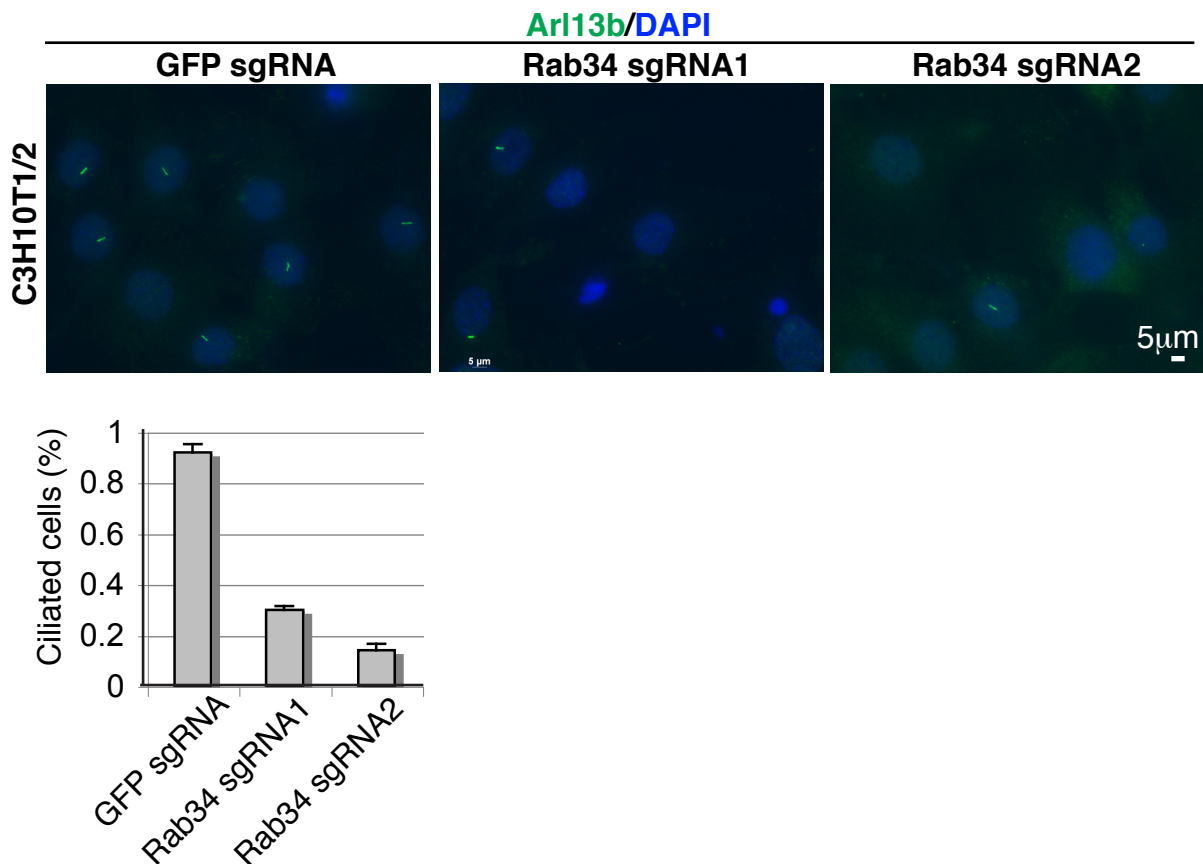**Figure S1**. A Rab34 CRISPR mutant allele.

Arl13b/**DAPI**

Figure S2. Loss of Rab34 in cultured cells results in a significant decrease in ciliogenesis. C3H10T1/2 cells were stably infected with Lentivirus that expressed sgRNAs as indicated. The cells were then immunostained for Arl13b, a ciliary marker, and counterstained for nuclei (DAPI). Two-tailed Student t-test P values ≤ 0.0001 (n = 3 independent experiments, ≥100 cells counted for each category).
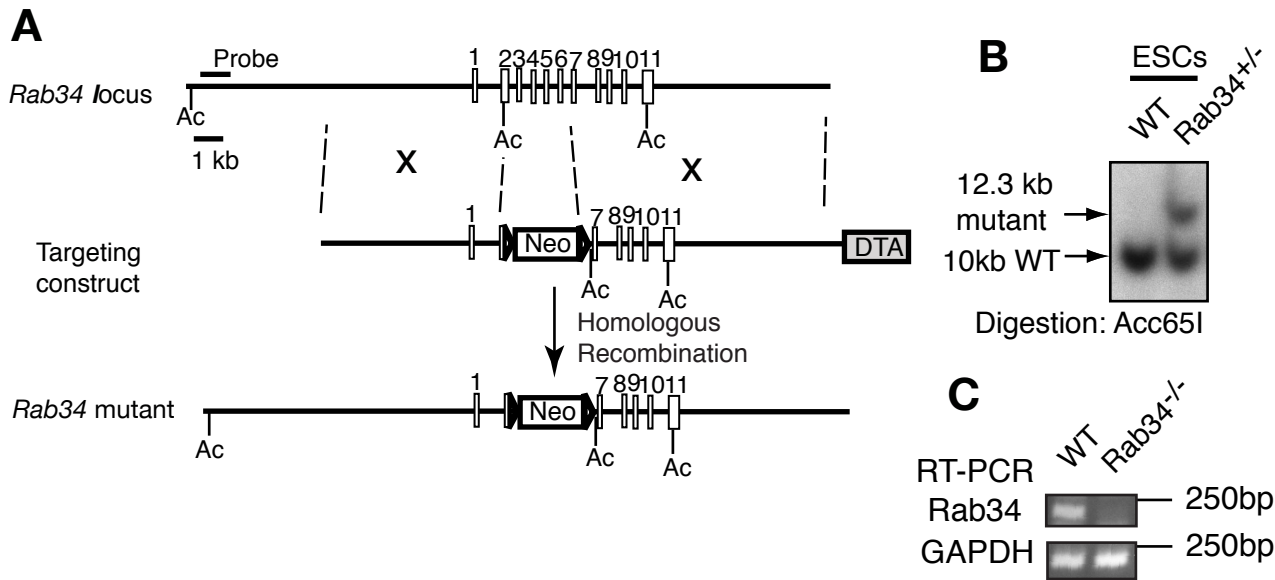
Figure S3. (A) The gene targeting strategy used to create a mouse Rab34 mutant allele. Open rectangles are referred to as exons and lines as introns. The probe used for Southern blot is shown. Triangle, loxP site; Neo, neomycin; DTA, diphtheria toxin A; number, exons; Ac, Acc65I. (B) Southern blot of representative mutant and wild type (wt) ES cell clones (n = 1 experiment). (C) RT-PCR shows that Rab34 transcript is undetectable in the mutant. GAPDH is a control.
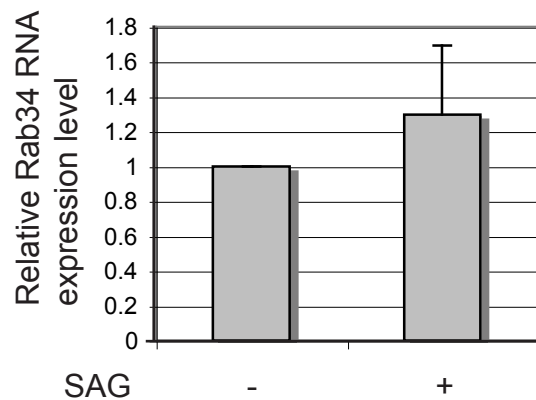

Figure S4. Activation of Hedgehog signaling does not significantly increase Rab34 RNA expression. RT-qPCR showing relative Rab34 RNA expression level in WT MEFs after stimulation with SAG. Two-tailed Student t-test p value is 0.176, not significant.

Table S1 Rab34 mutant E10.5 embryos

Phenotypes	Genotypes			
	+/+	+/-	-/-	Total
	11	24	10	45
Heart looping (left orientation)	11	24	10	45